Materials Today Bio 9 (2021) 100096

Contents lists available at ScienceDirect

Materials Today Bio

journal homepage: www.journals.elsevier.com/materials-today-bio

Platelet lysates-based hydrogels incorporating bioactive mesoporous silica nanoparticles for stem cell osteogenic differentiation

M.T. Tavares [a,b], S.C. Santos [a], C.A. Custódio [a], J.P.S. Farinha [b], C. Baleizão [b], J.F. Mano [a,*]

[a] CICECO - Aveiro Institute of Materials, Department of Chemistry, University of Aveiro, Aveiro, Portugal
[b] CQE - Centro de Química Estrutural, IN-Institute of Nanosciences and Nanotechnology, Instituto Superior Técnico, Universidade de Lisboa, Lisboa, Portugal

ARTICLE INFO

Keywords:
Nanocomposite
hBM-MSCs
Dexamethasone
Calcium and phosphate ions
Bone regeneration

ABSTRACT

Scaffolds for bone tissue regeneration should provide the right cues for stem cell adhesion and proliferation, but also lead to their osteogenic differentiation. Hydrogels of modified platelet lysates (PLMA) show the proper mechanical stability for cell encapsulation and contain essential bioactive molecules required for cell maintenance. We prepared a novel PLMA-based nanocomposite for bone repair and regeneration capable of releasing biofactors to induce osteogenic differentiation. Human bone marrow-derived mesenchymal stem cells (hBM-MSCs) were encapsulated in PLMA hydrogels containing bioactive mesoporous silica nanoparticles previously loaded with dexamethasone and functionalized with calcium and phosphate ions. After 21 d of culture, hBM-MSCs remained viable, presented a stretched morphology, and showed signs of osteogenic differentiation, namely the presence of significant amounts of alkaline phosphatase, bone morphogenic protein-2 and osteopontin, hydroxyapatite, and calcium nodules. Developed for the first time, PLMA/MSNCaPDex nanocomposites were able to guide the differentiation of hBM-MSCs without any other osteogenic supplementation.

1. Introduction

Bone is a living organ with a very complex structure that includes different cell types (e.g. osteoblasts, osteoclasts, mesenchymal stem cells) and several structural proteins (e.g. collagen) and proteoglycans [1–3]. Although bone has a self-healing ability, the healing of critical size fractures may require assisted bone repair. Autologous and allogeneic bone grafts are the current treatments, but both present disadvantages such as rejection, donor's morbidity, and inflammation [2]. As an alternative, tissue engineering combines biomaterials, cells, and bioactive factors to fabricate substitutes that mimic the native bone tissue. The combination of polymers with inorganic elements has been explored to better mimic the composite native structure of bone tissue [2,4].

Three-dimensional (3D) cell culture platforms have been emerging in order to enhance the similarities with extracellular matrix (ECM) and native tissue microenvironment [5]. Within such 3D structures, hydrogels have been widely explored in tissue engineering applications because of their physical and biological properties that are comparable to those of the ECM [6,7]. Unlike other hydrogels, platelet lysates (PL)-based hydrogels provide a high content of bioactive molecules, such as cytokines and growth factors, involved in cell growth and proliferation [8,9]. Because PL-based hydrogels usually suffer from poor mechanical properties and poor stability *in vitro*, new approaches have emerged in order to overcome these issues [8,10]. Examples are loading or incorporation of PL in scaffolds [11–13], use of cross-linking agents (e.g. genipin) [14], or PL modification with cross-linkable groups [9]. PL has the advantage of being cost-effective, easily available, and from human origin. They can, thus, be used as an allogeneic or autologous material to locally enhance healing processes [8,11]. Moreover, PL and platelet-rich plasma (PRP) have been used for several applications, including chondrogenic [11,15] and osteogenic differentiation [16,17], or ischemia [18]. In a recent study, photocrosslinkable PL-based hydrogels were obtained by conjugating PL proteins with methacryloyl groups (PLMA) [9]. Such hydrogels were proved to have increased and tunable mechanical properties and higher stability than PL-based hydrogels previously reported. PLMA hydrogels have shown to support distinct human-derived cell cultures, namely human mesenchymal stem cells, osteoblasts, and different bone osteosarcoma cell lines. Remarkably, encapsulated cells could also perform important biological processes such as growth, sprouting, and migration [9,19].

By incorporating nanomaterials, nanocomposite hydrogels hold specific advantages from both components showing enhanced biological and physical properties that better mimic the *in vivo* microenvironment [20,21]. Inspired by hybrid natural structures [22], nanocomposite hydrogels

* Corresponding author.
E-mail address: jmano@ua.pt (J.F. Mano).

https://doi.org/10.1016/j.mtbio.2021.100096
Received 9 November 2020; Accepted 17 January 2021
Available online 23 January 2021

using silica nanoparticles have been used to induce osteogenic differentiation of human stem cells [23,24]. More specifically, mesoporous silica nanoparticles (MSNs) have been shown to be very efficient nanocarriers because of their large surface area and pore volume and available surface for functionalization [25–29]. The organic/inorganic conjugation leads to an advantageous release system with enhanced bioactivity when compared to their individual counterparts [7,30].

Calcium ions are known to stimulate osteoblast proliferation and differentiation, while phosphate ions enhance mineral deposition in bone and are directly involved in bone matrix production by osteoblasts [1, 31]. Nanoparticles containing both ions are bioactive, contributing to a strong bond between the bone and the implant, by the formation of a hydroxyapatite layer [32]. The bioactivity of these nanoparticles can be further improved if they can release dexamethasone (Dex), which has osteoconductive properties and is also directly involved in osteogenic differentiation. Toxic side-effects of Dex at high concentrations require the use of controlled release drug delivery systems for improved effectiveness and safety [33–35].

In an attempt to take advantage of all great features of both PLMA hydrogels and MSNs, the goal of this work was to prepare a nanocomposite PLMA-based hydrogel to function not only as support for stem cell attachment and growth, but also to induce differentiation without the need of osteogenic supplementation. Our strategy (Fig. 1) starts by preparing MSNs functionalized with calcium (Ca^{2+}) and phosphate ions (PO_4^{3-}) on the external surface and loaded with Dex (MSNCaPDex). These MSNCaPDex were incorporated in PLMA hydrogels along with human bone marrow mesenchymal stem cells (hBM-MSCs) to form the final nanocomposite hydrogel. hBM-MSCs have been extensively studied in bone tissue regeneration because of their known capacity to differentiate into bone cells and also because of their availability [36]. Here we report for the first time the use of PLMA-based hydrogel nanocomposites with MSNCaPDex for osteogenic differentiation. This novel nanocomposite material is expected to have the proper biochemical microenvironment and bioactive content to modulate the fate of encapsulated cells without any further input, thus facilitating its future use in *in vivo* implantation.

2. Materials and methods

2.1. Materials

Tetraethylorthosilicate (TEOS, 98%, Merck-Sigma, Germany), N-cetyltrimethylammonium bromide (CTAB, 99%, Merck-Sigma), sodium hydroxide (NaOH, Merck-Sigma), absolute ethanol (99.9%, Scharlab, Spain), calcium hydroxide ($Ca(OH)_2$, ≥95%, Merck-Sigma), diammonium hydrogen phosphate (DHP, $(NH_4)_2HPO_4$, 98%, Merck-Sigma), Dex (Dex, Thermo Fisher Scientific, USA), human PL (STEMCELL Technologies, Canada), methacrylic anhydride (MA) (94%, Sigma-Aldrich, Germany), 2-hydroxy-4'-(2-hydroxyethoxy)-2 methylpropiophenone (Irgacure 2959, Sigma-Aldrich), polydimethylsiloxane (PDMS, Dow Corning, USA), phosphate-buffered saline (PBS, Thermo Fischer Scientific, USA), perylene-diimide (PDI), Minimum Essential Medium Alpha (MEM-α) (Thermo Fisher Scientific), fetal bovine serum (FBS, Thermo Fisher Scientific), antibiotic/antimycotic (Thermo Fisher Scientific), trypsin/EDTA (0.25%, Sigma-Aldrich), L-ascorbic acid (Sigma-Aldrich), β-glycerophosphate (Sigma-Aldrich), calcein AM ($4x10^{-3}$ M in DMSO, Thermo Fisher Scientific), propidium iodide (Thermo Fisher Scientific), Quant-iT PicoGreen dsDNA Assay Kit (Thermo Fisher Scientific), *p*-Nitrophenyl phosphate (pNPP, -Merck-Sigma), Triton X-100 (Sigma-Aldrich), bovine serum albumin (BSA, Sigma-Aldrich), mouse anti-human osteopontin (OPN) antibody (Biolegend, USA), Alexa Fluor 488 goat anti-mouse (Biolegend), 4′,6′-diamino-2-fenil-indol (DAPI, Thermo Fisher Scientific), OsteoImage™ Mineralization Assay kit (Lonza, Switzerland), Alizarin Red S (Sigma-Aldrich).

2.2. Synthesis of bioactive mesoporous silica nanoparticles

MSNs were produced based on a previously described procedure [37]. Briefly, in a polypropylene flask, 240 mL of Milli-Q water were mixed with 1.75 mL of NaOH (1.7 M) at 40 °C. Once the temperature stabilized, 0.5 g of CTAB was added. After 30 min stirring, 2.5 mL of TEOS was added dropwise, and the reaction was left to proceed for 2 h. After cooling to room temperature (RT), the dispersion was centrifuged (30,000 g, 20 min) and washed three times with 50% (v/v) ethanol. The particles were then dried at 50 °C in a ventilated oven. Afterward, MSNs were functionalized with Ca^{2+} and PO_4^{3-} ions and loaded with Dex to form MSNCaPDex, as described elsewhere [38]. Briefly, after MSNs dispersion in milli-Q water, solutions of $Ca(OH)_2$ (0.15 g L^{-1}) and DHP (0.10 g L^{-1}) were added to the dispersion and the mixture was stirred overnight at RT. For recovery, the dispersion was centrifuged and MSNCaP were washed three times with milli-Q water and dried at 50 °C. To remove the template, the particles were finally calcinated at 550 °C for 6 h. For the incorporation of Dex, 100 mg of MSNCaP and 4 mg of Dex were mixed in 0.4 mL of ethanol, and the mixture was stirred for 24 h at RT. The nanoparticles were collected by centrifugation and washed with

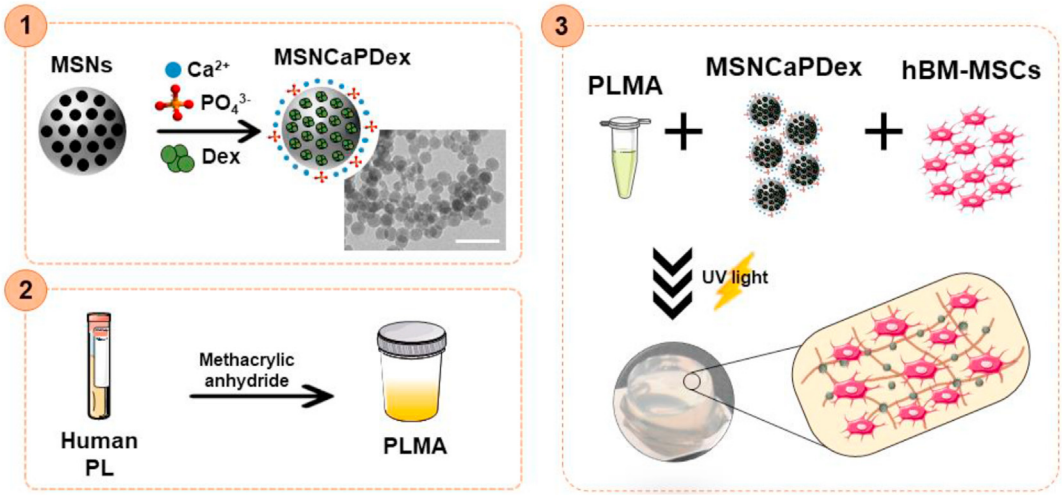

Fig. 1. Schematic representation of the nanocomposite hydrogel production. (1) Synthesis of bioactive mesoporous silica nanoparticles (MSNCaPDex): mesoporous silica nanoparticles (MSNs) were functionalized with calcium (Ca^{2+}) and phosphate ions (PO_4^{3-}) and loaded with dexamethasone (Dex) to form MSNCaPDex. Scale bar: 200 nm (2) Modified platelet lysates (PLMA) were synthesized by reaction of platelet lysates (PL) with methacrylic anhydride. (3) Nanocomposite PLMA hydrogels production by mixing MSNCaPDex and human bone marrow mesenchymal stem cells (hBM-MSCs) in a PLMA solution followed by UV light irradiation in order to form the hydrogels.

TRIS-buffer solution (10 mM TRIS, 0.17 M NaCl, pH 7.4) three times.

2.3. PLMA hydrogel nanocomposite preparation

PLMA were synthesized using a previously reported procedure [9]. Briefly, human PL was chemically modified by reaction with MA. The excess MA was removed by dialysis against deionized water, and the PLMA freeze-dried and kept at 4 °C until further use. Lyophilized PLMA was dissolved in a solution of 0.5% (w/v) Irgacure 2959 in PBS to a final concentration of 15% (w/v) PLMA. Afterward, MSNCaPDex was mixed in 15% (w/v) PLMA solution to a final concentration of 1% (w/v) nanoparticles. PLMA hydrogel nanocomposite was prepared by transferring the solution to PDMS molds with 6 mm diameter followed by ultraviolet (UV) irradiation (95 mW cm^{-2}).

To assess MSNCaPDex dispersion in the PLMA hydrogel composites, a fluorescent molecule (PDI) was incorporated in the nanoparticles structure (PDI-MSNCaPDex), as previously reported [25]. PLMA hydrogel nanocomposites with PDI-MSNCaPDEx were imaged in an upright fluorescence microscope (Zeiss Imager M2) equipped with a monochromatic digital camera (AxioCam MRm, 3Mpix). Image processing was performed with the ZEN v2.3 blue edition software (Carl Zeiss Microscopy GmbH).

2.4. Rheological studies

Elastic and viscous moduli of PLMA and PLMA nanocomposite solutions during the photopolymerization process were studied by photorheology. Both 15% (w/v) PLMA and 15% (w/v) PLMA containing 1% (w/v) MSNCaPDex were used for rheological studies. A Kinexus Lab+ (Malvern Panalytical, UK) equipped with a UV curing attachment was used to characterize the photocrosslinking kinetics. The gap setting was fixed as 0.5 mm, and light intensity (95 mW/cm^2) was used for the crosslinking reaction of the precursor. Tests were performed at 25 °C with a frequency of 1.0 Hz and 0.02% of shear strain.

2.5. Compressive mechanical tests

The mechanical behavior of PLMA hydrogels at 15% (w/v) and PLMA hydrogels at 15% (w/v) containing 1% (w/v) of MSNCaPDex was assessed by compression testing using a Instron Uniaxial Testing Machine (Instron, US) equipped with a 50 N load cell. Unidirectional compression assays were performed on fresh-prepared cylindrical hydrogels (6 mm of diameter and 2.5 mm of height) at RT. The Young's modulus was defined as the slope of the linear region (0–5% of strain) of the strain-stress curve.

2.6. In vitro cell culture-and hBM-MSCs encapsulation

hBM-MSCs (hBM-MSCs, ATCC, USA) were cultured in MEM-α supplemented with 10% FBS and 1% antibiotic/antimycotic. The cells were cultured under standard conditions (5% CO_2 atmosphere at 37 °C). The medium was replaced every 2 d, and the cells were used until passage 6. hBM-MSCs suspensions were prepared by trypsinization (0.25% trypsin/EDTA solution).

For *in vitro* cell tests, PLMA hydrogels with hBM-MSCs encapsulated were produced with and without MSNCaPDex. MSNCaPDex was previously sterilized with ethanol for 2 h and afterward resuspended in the PLMA solution. For all conditions, the cells were resuspended in PLMA precursor solutions to a final density of 4×10^6 cells mL^{-1}. PLMA hydrogels with and without MSNCaPDex were produced as described previously. PLMA hydrogels without MSNCaPDex were culture in both basal medium – MEM-α and osteogenic medium – MEM-α supplemented with ascorbic acid (10×10^{-3} M), Dex (100×10^{-9} M) and β-glycerophosphate (50 μg mL^{-1}). PLMA hydrogel nanocomposites were cultured only in basal medium. The cells were incubated, and at pre-determined time points (1, 7, 14, and 21 d), their viability, proliferation and differentiation were assessed.

2.7. Live/dead assay

At predetermined time points, PLMA hydrogels were incubated in a solution of 2 μL of calcein AM 4×10^{-3} M solution in DMSO and 1 μL of propidium iodide 1 mg mL^{-1} in 1,000 μL of PBS at 37 °C during 30 min. After washing with PBS, hydrogels were examined using an upright fluorescence microscope (Zeiss Imager M2) equipped with a monochromatic digital camera (AxioCam MRm, 3Mpix). Image processing was performed by using the ZEN v2.3 blue edition software (Carl Zeiss Microscopy GmbH).

2.8. Cell proliferation quantification

Double-strained DNA (dsDNA) quantification assay (Quant-iT PicoGreen dsDNA Assay Kit) was performed to follow cell proliferation. In specific time points, the culture media were removed, and the hydrogels washed with PBS. The hydrogels were immersed in sterilized deionized water and frozen at −80 °C. The samples were thawed at 37 °C and sonicated for 30 min to induce complete membrane disruption. DNA standards were prepared with concentrations ranging between 0 and 1 μg mL^{-1}. The microplate was incubated in the dark for 10 min, and fluorescence was measured (480 nm excitation and 528 nm emission) in a microplate reader (Microplate Reader - Synergy HTX with luminescence, fluorescence and absorbance, BioTek Instruments, USA).

2.9. ALP activity measurement

ALP activity was quantified by the specific conversion of *p*-Nitrophenyl phosphate (pNPP) into *p*-Nitrophenol (pNP) using the same samples used for the DNA quantification. After thawing the samples at 37 °C, 60 μL of buffer solution containing 2 mg mL^{-1} pNPP was added to 20 μL of the supernatant in a 96-well plate. The enzyme reaction was carried out at 37 °C in the dark for 1 h and then stopped by adding 80 μL of the stop solution (3 M NaOH in deionized water). The absorbance was measured at 405 nm in a microplate reader (Microplate Reader - Synergy HTX with luminescence, fluorescence, and absorbance, BioTek Instruments, USA). A standard curve was extrapolated by using pNP values ranging from 0 to 0.5 mM. The ALP values are normalized to the dsDNA content.

2.10. BMP-2 quantification by ELISA

The amount of bone morphogenic protein 2 (BMP-2) released by the encapsulated cells was assessed by ELISA quantification assay. For that, the supernatants (1 mL) of cell culture media at 21 d of culture were stored at −80 °C until analysis. Commercially available human BMP-2 ELISA development kits (Abcam) were performed according to the manufacture's specifications. The measurements were read at 450 nm in a microplate reader (Microplate Reader - Synergy HTX with luminescence, fluorescence, and absorbance, BioTek Instruments, USA).

2.11. Osteopontin immunostaining

The expression of OPN on the PLMA hydrogels was assessed after 21 d of culture by fluorescence imaging. After wash with PBS, the hydrogels were fixed with 10% (v/v) formalin for 2 h. The samples were then permeabilized with 1% (v/v) Triton X-100 in PBS, blocked with 3% (w/v) BSA during 1 h and incubated overnight with mouse anti-human OPN antibody (1:100 in 5% (v/v) FBS/dPBS) at 4 °C. Cells were then rinsed in PBS and incubated with Alexa Fluor 488 goat anti-mouse (1:400 in 5% (v/v) FBS/dPBS) for 1 h at RT in the dark. For cell nucleus staining, the samples were incubated for 5 min with DAPI (1:1000 in PBS, original solution at 5 mg mL^{-1}). After washing with PBS, hydrogels were examined using an upright fluorescence microscope (Zeiss Imager M2) equipped with a monochromatic digital camera (AxioCam MRm, 3Mpix). Image processing was performed by using the ZEN v2.3 blue edition

software (Carl Zeiss Microscopy GmbH).

2.12. Biomineralization analysis

In vitro biomineralization was assessed at 21 d of culture either by hydroxyapatite crystals analysis or Alizarin Red S staining. In order to detect hydroxyapatite crystal, OsteoImage™ Mineralization Assay kit was used according to the manufacturer's instructions. After fixation with 10% (v/v) formalin, the samples were incubated with Osteoimage™ Staining reagent (1:100 in PBS) for 30 min. Afterward, the samples were incubated for 5 min with DAPI (1:1000 in PBS, original solution at 5 mg mL^{-1}). After washing with PBS, hydrogels were examined using an upright fluorescence microscope (Zeiss Imager M2) equipped with a monochromatic digital camera (AxioCam MRm, 3Mpix). Image processing was performed by using the ZEN v2.3 blue edition software (Carl Zeiss Microscopy GmbH). For Alizarin Red S mineralization assay, hydrogels were fixed and washed as previously mentioned. After, the samples were incubated with 1 mL of Alizarin Red S (4×10^{-4} M, pH 4.2) for 1 h at RT. The staining solution was then removed, and the cells rinsed three times with PBS. The images were acquired using a Stemi 508 Stereo Microscope (Zeiss).

2.13. Statistical analysis

Data are presented as mean ± standard deviation in each experiment. The statistical analysis was performed by using the two-way ANOVA with post hoc Tukey's multiple comparisons tests, using GraphPad Prism v6.00 software (San Diego, USA). Statistical significance was defined at $p<0.05$ for a 95% confidence interval. For mechanical and rheological results, Unpaired *t*-test with 99% confidence were performed, using the same software.

3. Results and discussion

3.1. Nanocomposite PLMA hydrogel formulation and characterization

We hypothesize that the bioactive MSNs containing Ca^{2+}, PO_4^{3-} and Dex (MSNCaPDex) will be efficient in leading hBM-MSCs osteogenic differentiation when combined with PLMA in a 3D system. For proof-of-concept, we developed a novel PLMA hydrogel nanocomposite by incorporating 1% (w/v) bioactive MSNCaPDex.

MSNCaPDex nanoparticles labeled with a fluorescent dye (PDI) were dispersed in a PLMA solution prior to photocrosslinking. The obtained hydrogel nanocomposites were observed by fluorescence microscopy, showing that MSNCaPDex are well distributed inside the PLMA hydrogels – see Fig. 2A.

The mechanical properties of the PLMA hydrogel nanocomposites were obtained from compression tests. The Young's modulus, defined as the slope of the linear region (0–5% of strain) of the strain–stress curve, shows that there are no significant differences between the stiffness value of PLMA hydrogels and nanocomposite PLMA hydrogels, meaning that the presence of nanoparticles did not affect the mechanical behavior of PLMA hydrogels (Fig. 2B). In particular, we can conclude that the addition of 1% (w/v) of the silica-based nanoparticles did not produce a significant change in the stiffness of the hydrogel. For the assessment of the rheological properties, photo-rheological measurements were performed. Fig. 2C shows a representative curve of the storage modulus (G′) for both conditions studied. Fig. 2D shows the results obtained for $t_{1/2}$,

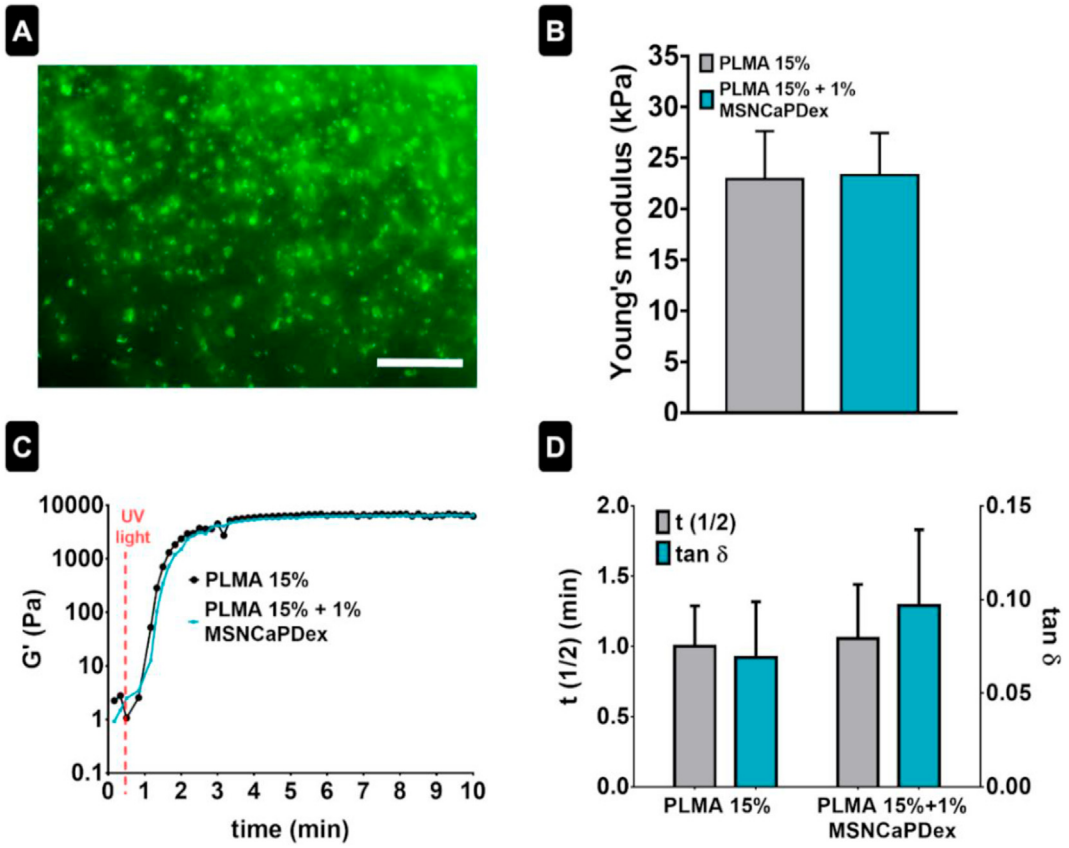

Fig. 2. PLMA/MSNCaPDex nanocomposites characterization. (A) MSNCaPDex labeled with PDI dispersion in PLMA hydrogel. Scale bar: 100 μm (B) Young's modulus for PLMA without and with 1% MSNCaPDex. (C) Representative curves for storage modulus (G′) and (D) $t_{1/2}$ and tan δ for PLMA 15% and PLMA 15% + 1% MSNCaPDex. Statistical analysis by *unpaired t-test* with a 99% confidence showed no significant differences.

which gives the time where G′ reach the average value of the storage moduli of the hydrogel and the liquid sample, and tan δ, which gives the ratio between loss modulus (G″) and G'. It can be observed there are no significant differences for such values between both conditions studied. Both the photocrosslinking time and the viscoelastic nature of the hydrogels are maintained even in the presence of MSNCaPDex.

3.2. Cellular viability assay

PLMA hydrogels have been shown to adequately support human stem cell adhesion and proliferation [9,19]. Before studying the effect of the presence of MSNCaPDex on stem cells differentiation, we evaluated the viability and adhesion of hBM-MSCs in the new PLMA hydrogel nanocomposite. hBM-MSCs were encapsulated in PLMA and PLMA-MSNCaPDex hydrogels for 14 d. For PLMA hydrogels, here used as controls, the cell culture was performed in basal medium (MEM-α) and osteogenic medium (MEM-α supplemented with ascorbic acid, Dex, and β-glycerophosphate). In the case of nanocomposite PLMA hydrogels, only basal medium was used during cell culture time. At pre-determined time points, namely 1, 7, and 14 d of culture, a live/dead assay was performed in order to access cell viability inside PLMA and PLMA/MSNCaPDex hydrogels. Fig. 3 shows the representative fluorescence images for live/dead assays for all the conditions studied. After 24 h, the cells remain viable inside both PLMA and PLMA hydrogels nanocomposite. After 2 weeks, hBM-MSCs are viable and perfectly spread inside the hydrogels. This proves that the presence of the nanoparticles does not affect the viability of the cells, but also that the hBM-MSCs were able to adhere and spread within the 3D PLMA matrix.

3.3. hBM-MSCs osteogenic differentiation

The capacity of MSNCaPDex to induce the osteogenic differentiation of hBM-MSCs was already proved in a two-dimensional (2D) study, with several signs of differentiation after 21 d even without additional osteogenic supplementation [38]. The incorporation and release of Dex and calcium and phosphate ions were also evaluated previously [38,39]. The concentration of bioactive factors released proved to be enough to induce an osteogenic response in hBM-MSCs with a single-dose administration. However, 2D cultures do not replicate the *in vivo* cell microenvironment [5]. In the present work, the goal was to understand the ability of MSNCaPDex to induce osteogenic differentiation of hBM-MSCs when incorporated in a 3D structure, which can better mimic the native ECM and its mechanical and biochemical signals [9]. Similarly to the live/-dead studies, hBM-MSCs were encapsulated in the studied hydrogels. It is important to note that half of the medium was exchanged every 3 d. Basal medium was used for experiments with nanocomposites and for the negative control, while osteogenic medium was used for the positive control, meaning that the latter was supplemented with fresh osteogenic factors every 3 d, while the nanocomposite did not receive further osteogenic factors.

To understand if hBM-MSCs were able to differentiate inside PLMA hydrogels, specific osteogenic markers were quantified: ALP and human recombinant BMP-2. ALP is a membrane-bound enzyme synthesized earlier on the osteogenic differentiation pathway, and it is related with matrix mineralization and thus bone synthesis [1,40]. BMP-2 is involved in osteogenic differentiation modulation and coordinates bone formation [41]. From 7 to 14 d of culture, there is an increase in ALP in the presence of MSNCaPDex, with values significantly higher than the basal medium and comparable to the osteogenic medium – see Fig. 4A. At day 21, the cells in the presence of osteogenic medium reach the maximum of ALP

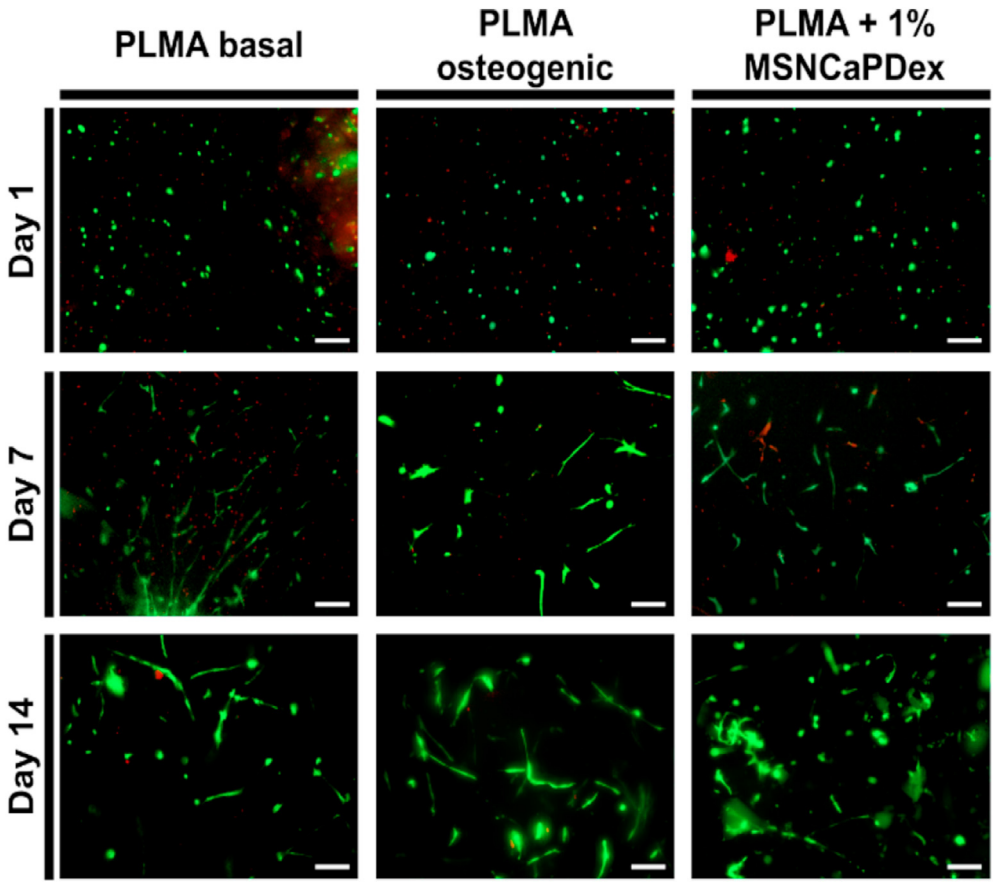

Fig. 3. Live/dead assays. Representative live/dead images of hBM-MSCs encapsulated in PLMA hydrogels (cultured in basal and osteogenic medium) and encapsulated in PLMA hydrogel nanocomposites (cultured in basal medium), at 1, 7, and 14 d of culture. Scale bar: 200 μm.

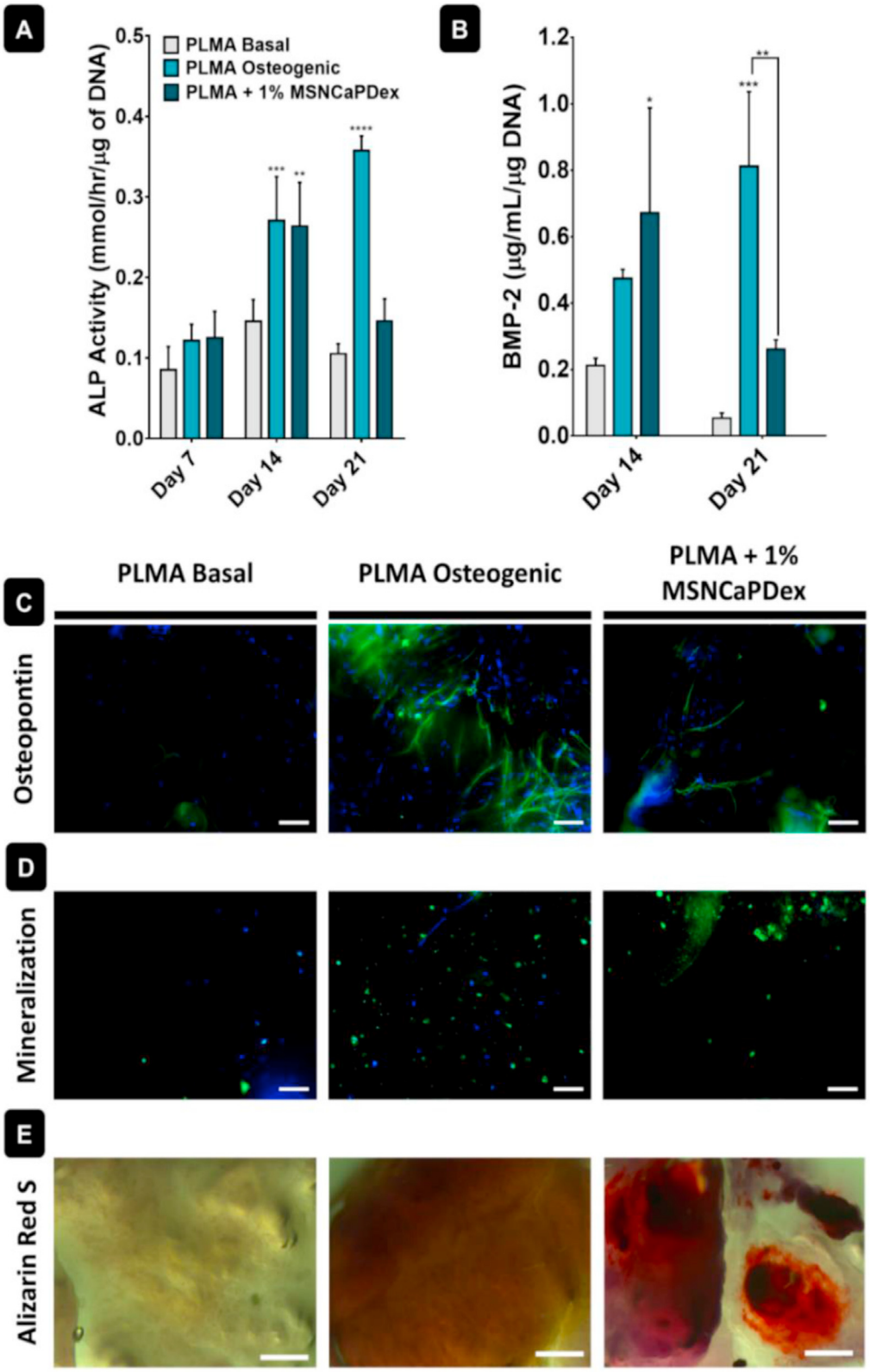

Fig. 4. Study of osteogenic differentiation for hBM-MSCs encapsulated in PLMA hydrogels cultured with basal medium, osteogenic medium, and 1% MSNCaPDex PLMA hydrogels in basal medium. *In vitro* (A) ALP activity and (B) BMP-2 quantification. Representative fluorescence images after 21 d of: (C) osteopontin (green channel: Alexa Fluor 488, osteopontin staining; blue channel: DAPI, nucleus staining) and (D) hydroxyapatite (green channel: hydroxyapatite staining; blue channel: DAPI, nucleus staining). Scale bar: 100 μm. (E) Representative optical microscopy images of Alizarin Red S staining of calcium deposits after 21 d. Scale bar: 500 μm. Data represent mean ± s.d. (n = 3). * = $p<0.05$, ** = $p<0.01$, *** = $p<0.001$, **** = $p<0.0001$. Symbols above bars are compared to those of basal medium.

production, while there is a decrease in the presence of MSNCaPDex. Similarly to ALP, the maximum concentration of BMP-2 in the presence of MSNCaPDex is reached after 14 d (Fig. 4B), with values significantly higher than those obtained with nanoparticles in basal medium and comparable to those in osteogenic medium. The results also demonstrate a decrease in both ALP and BMP-2 concentration from 14 to 21 d of culture for PLMA + MSNCaPDex, unlike what happens for PLMA in the osteogenic medium. This is probably due to the fact that more osteogenic factors were added every time the osteogenic medium was replaced, while in PLMA + MSNCaPDex, the quantity of these factors is dependent only on the amount initially present in the MSNCaPDex.

hBM-MSCs osteogenic differentiation was also evaluated by analyzing the extracellular deposition of mineralized matrix. First, OPN immunostaining was performed, as this is a bone-associated protein involved in bone mineralization and a key factor in bone remodeling [35]. Fig. 4C shows representative fluorescence images of OPN immunostaining after 21 d of culture. Images show the presence of OPN in cells encapsulated in the PLMA hydrogels cultured in osteogenic medium and in hydrogel nanocomposites. For PLMA hydrogels cultured in basal medium, no signs of OPN staining were found.

The performance of the PLMA hydrogels nanocomposites was also investigated by hydroxyapatite immunostaining and alizarin red S staining, for calcium nodules. Hydroxyapatite-based microcrystals are deposited into the collagen matrix of bone and therefore are an important marker of osteogenic differentiation [1]. Hydroxyapatite formation was assessed by fluorescence microscopy, and it is possible to observe higher amounts of hydroxyapatite either in PLMA hydrogels cultured in osteogenic medium or in PLMA hydrogel nanocomposites cultured in basal medium (Fig. 4D). Alizarin red S staining was used to observe the calcium nodules formed by the cells. There is a clear difference in the formation of calcium nodules between the PLMA hydrogels cultured in basal medium and the other two conditions (Fig. 4E), meaning that calcium deposition only occurred in PLMA hydrogels in osteogenic medium or in the PLMA hydrogel nanocomposites.

Regarding the efficacy of our nanocomposite hydrogel, the most correct comparison should be made with the negative control, as both are cultured in basal medium. In that case, both ALP and BMP-2 production is significantly higher at day 14, and the presence of OPN, hydroxyapatite, and calcium nodules is only observed in the PLMA-MSNCaPDex hydrogels.

Overall, our results suggest that hBM-MSCs in PLMA hydrogels do not show any signs of differentiation when cultured in basal medium. This follows previous results where the addition of PL to a dextran scaffold did not lead to osteoblast differentiation *in vitro* [11]. The secretion of osteocalcin was detected with the addition of PL to a chitosan-based scaffold, but there was no mineralization at day 21 [16]. In this study, the similarity of the results obtained for the cells in osteogenic medium and in PLMA/MSNCaPDex hydrogels is evident. The main difference between these conditions is that hBM-MSCs cultured in osteogenic medium were supplemented every 3 d with osteogenic enhancers due to the medium exchange, while the hBM-MSCs encapsulated in PLMA hydrogel nanocomposites were cultured in basal medium. However, the maximum values of ALP and BMP-2 production are reached at an earlier time point when MSNCaPDex is used. This means that the bioactive factors released from the MSNCaPDex are enough to reach comparable production of bone-associated markers and similar levels of mineralization to the positive control without the need for further supplementation. Previous studies with nanocomposite scaffolds using bioactive MSNs showed an effect in osteogenic differentiation in the presence of the nanoparticles, but using osteogenic or osteoconductive medium [42–44]. Contrarily to most studies, this work is conducted in basal medium, so instead of looking only for a possible upregulation of osteogenic differentiation, here we prove that the presence of MSNCaPDex in PLMA hydrogels is enough to reach a similar response to the osteogenic medium. Overall, by combining the easy availability of human bioactive PL with osteoinductive nanoparticles, we obtain a nanocomposite hydrogel ideal for bone tissue regeneration.

4. Conclusions

For the first time, hydrogels based on human PL were combined with osteoinductive nanoparticles to engineer a multifunctional bioactive system for bone tissue engineering. Bioactive silica nanoparticles, MSNCaPDex, were incorporated in PLMA hydrogels in order to obtain a nanocomposite material able to support stem cell culture and migration and also to induce their differentiation to the osteogenic lineage. MSNCaPDex was dispersed in the hydrogel matrix and did not affect the PLMA hydrogels mechanical properties or cell viability. Most importantly, the presence of 1% MSNCaPDex was enough for hBM-MSCs to reach high levels of ALP and BMP-2 and to produce OPN, hydroxyapatite, and calcium nodules associated with the process of differentiation. The results from this study show that the presence of MSNCaPDex in PLMA hydrogels produces a similar response to that obtained using continuous osteogenic supplementation. Therefore, the use of the hydrogel nanocomposites is an extremely attractive alternative to the repeated delivery of osteogenic factors, simplifying the procedure by releasing them in a more controlled manner. By combining a brand-new hydrogel that shows so many advantages for cell culture with a bioactive nanomaterial proven to be efficient on its own, we obtain a suitable PLMA-MSNCaPDex hydrogel for bone tissue regeneration. This could be relevant in applications where we wish to induce cell's differentiation within the implantable device. We hypothesize that such intrinsically osteogenic hydrogels could be delivered either by injection or surgery and could accelerate bone regeneration *in situ*.

Declaration of competing interest

The authors declare that they have no known competing financial interests or personal relationships that could have appeared to influence the work reported in this paper.

Acknowledgments

This work was supported by Fundos Europeus Estruturais e de Investimento (FEEI), Programa Operacional Regional de Lisboa-FEDER (02/SAICT/2017), and national funds from Fundação para a Ciência e a Tecnologia (FCT-Portugal) and COMPETE (FEDER) within projects UIDB/00100/2020 and UIDP/00100/2020 (CQE), PTDC/CTM-POL/3698/2014, PTDC/CTM-CTM/32444/2017 (02/SAICT/2017/032444) and Margel (PTDC/BTM-MAT/31498/2017). This work was developed within the scope of the project CICECO-Aveiro Institute of Materials, UIDB/50011/2020 and UIDP/50011/2020, financed by national funds through the Portuguese Foundation for Science and Technology/MCTES. M. Tavares also thanks FCT for a PhD grant (FCT-PD/BD/114019/2015).

References

[1] H.C. Blair, Q.C. Larrouture, Y. Li, et al., Osteoblast differentiation and bone matrix formation in vivo and in vitro, Tissue Eng. Part B 23 (2017) 268–280, https://doi.org/10.1089/ten.teb.2016.0454.

[2] D.L. Lopes, C. Martins-Cruz, M.B. Oliveira, J.F. Mano, Bone physiology as inspiration for tissue regenerative therapies, Biomaterials 185 (2018) 240–275, https://doi.org/10.1016/j.biomaterials.2018.09.028.

[3] N. Reznikov, R. Shahar, S. Weiner, Bone hierarchical structure in three dimensions, Acta Biomater. 10 (2014) 3815–3826, https://doi.org/10.1016/j.actbio.2014.05.024.

[4] J.F. Mano, Designing biomaterials for tissue engineering based on the deconstruction of the native cellular environment, Mater. Lett. 141 (2015) 198–202, https://doi.org/10.1016/j.matlet.2014.11.061.

[5] K. Duval, H. Grover, L.-H. Han, et al., Modeling physiological events in 2D vs 3D cell culture, Physiology 32 (2017) 266–277, https://doi.org/10.1152/physiol.00036.2016.

[6] A.K. Gaharwar, N.A. Peppas, A. Khademhosseini, Nanocomposite hydrogels for biomedical applications. Biotechnology and bioengineering, Biotechnol. Bioeng. 111 (2014) 441–453, https://doi.org/10.1002/bit.25160.

[7] S. Yang, J. Wang, H. Tan, F. Zeng, C. Liu, Mechanically robust PEGDA-MSNs-OH nanocomposite hydrogel with hierarchical meso-macroporous structure for tissue engineering, Soft Matter 8 (2012) 8981–8989, https://doi.org/10.1039/c2sm25123j.

[8] S.C. Santos, Ó.E. Sigurjonsson, C.A. Custódio, J.F. Mano, Blood plasma derivatives for tissue engineering and regenerative medicine therapies, Tissue Eng. B Rev. 24 (2018) 454–462, https://doi.org/10.1089/ten.TEB.2018.0008.
[9] S.C. Santos, C.A. Custódio, J.F. Mano, Photopolymerizable platelet lysate hydrogels for customizable 3D cell culture platforms, Adv Healthc Mater 7 (2018) 1–12, https://doi.org/10.1002/adhm.201800849.
[10] T. Burnouf, H.A. Goubran, T.-M. Chen, K.-L. Ou, M. El-Ekiaby, M. Radosevic, Blood-derived biomaterials and platelet growth factors in regenerative medicine, Blood Rev. 27 (2013) 77–89, https://doi.org/10.1016/j.blre.2013.02.001.
[11] L.S. Moreira Teixeira, J.C.H. Leijten, J.W.H. Wennink, et al., The effect of platelet lysate supplementation of a dextran-based hydrogel on cartilage formation, Biomaterials 33 (2012) 3651–3661, https://doi.org/10.1016/j.biomaterials.2012.01.051.
[12] J. Leotot, L. Coquelin, G. Bodivit, et al., Platelet lysate coating on scaffolds directly and indirectly enhances cell migration, improving bone and blood vessel formation, Acta Biomater. 9 (2013) 6630–6640, https://doi.org/10.1016/j.actbio.2013.02.003.
[13] C.R. Martins, C.A. Custódio, J.F. Mano, Multifunctional laminarin microparticles for cell adhesion and expansion, Carbohydr. Polym. 202 (2018) 91–98, https://doi.org/10.1016/j.carbpol.2018.08.029.
[14] R. Costa-Almeida, A.R. Franco, T. Pesqueira, et al., The effects of platelet lysate patches on the activity of tendon-derived cells, Acta Biomater. 68 (2018) 29–40, https://doi.org/10.1016/j.actbio.2018.01.006.
[15] E. Jooybar, M.J. Abdekhodaie, M. Alvi, A. Mousavi, M. Karperien, P.J. Dijkstra, An injectable platelet lysate-hyaluronic acid hydrogel supports cellular activities and induces chondrogenesis of encapsulated mesenchymal stem cells, Acta Biomater. 83 (2019) 233–244, https://doi.org/10.1016/j.actbio.2018.10.031.
[16] F. Re, L. Sartore, V. Moulisova, et al., 3D gelatin-chitosan hybrid hydrogels combined with human platelet lysate highly support human mesenchymal stem cell proliferation and osteogenic differentiation, J. Tissue Eng. 10 (2019) 1–16, https://doi.org/10.1177/2041731419845852.
[17] S.M. Oliveira, R.L. Reis, J.F. Mano, Assembling human platelet lysate into multiscale 3D scaffolds for bone tissue engineering, ACS Biomater. Sci. Eng. 1 (2015) 2–6, https://doi.org/10.1021/ab500006x.
[18] F. Saporito, L.M. Baugh, S. Rossi, et al., In situ gelling scaffolds loaded with platelet growth factors to improve cardiomyocyte survival after ischemia, ACS Biomater. Sci. Eng. 5 (2019) 329–338, https://doi.org/10.1021/acsbiomaterials.8b01064.
[19] C.F. Monteiro, S.C. Santos, C.A. Custódio, J.F. Mano, Human platelet lysates-based Hydrogels : a novel personalized 3D platform for spheroid invasion assessment, Adv. Sci. (2020) 1902398, https://doi.org/10.1002/advs.201902398.
[20] R. Tutar, A. Motealleh, A. Khademhosseini, N.S. Kehr, Functional nanomaterials on 2D surfaces and in 3D nanocomposite hydrogels for biomedical applications, Adv. Funct. Mater. 29 (2019) 1904344, https://doi.org/10.1002/adfm.201904344.
[21] Lavrador P, Gaspar VM, Mano JF. Stimuli-responsive Nanocomposite Hydrogels for Biomedical Applications. Advanced Functional Materials. (Accepted).
[22] G.M. Luz, J.F. Mano, Mineralized structures in nature: examples and inspirations for the design of new composite materials and biomaterials, Compos. Sci. Technol. 70 (2010) 1777–1788, https://doi.org/10.1016/j.compscitech.2010.05.013.
[23] A. Motealleh, N.S. Kehr, Nanocomposite hydrogels and their applications in tissue engineering, Adv Healthc Mater 6 (2017), https://doi.org/10.1002/adhm.201600938.
[24] A.J. Leite, J.F. Mano, Biomedical applications of natural-based polymers combined with bioactive glass nanoparticles, J. Mater. Chem. B 5 (2017) 4555–4568, https://doi.org/10.1039/c7tb00404d.
[25] T. Ribeiro, E. Coutinho, A.S. Rodrigues, C. Baleizão, J.P.S. Farinha, Hybrid mesoporous silica nanocarriers with thermovalve-regulated controlled release, Nanoscale 9 (2017) 13485–13494, https://doi.org/10.1039/C7NR03395H.
[26] A.S. Rodrigues, T. Ribeiro, F. Fernandes, J.P.S. Farinha, C. Baleizão, Intrinsically fluorescent silica nanocontainers: a promising theranostic platform, Microsc. Microanal. 19 (2013) 1216–1221, https://doi.org/10.1017/S1431927613001517.
[27] W. Cui, Q. Liu, L. Yang, et al., Sustained delivery of BMP-2-related peptide from the true bone ceramics/hollow mesoporous silica nanoparticles scaffold for bone tissue regeneration, ACS Biomater. Sci. Eng. 4 (2018) 211–221, https://doi.org/10.1021/acsbiomaterials.7b00506.
[28] C. Baleizão, J.P.S. Farinha, Hybrid smart mesoporous silica nanoparticles for theranostic, Nanomedicine 10 (2015) 1–7, https://doi.org/10.2217/nnm.15.102.
[29] J.L.M. Gonçalves, C.I.C. Crucho, S.P.C. Alves, C. Baleizão, J.P.S. Farinha, Hybrid mesoporous nanoparticles for pH-actuated controlled release, Nanomaterials 9 (2019) 1–13, https://doi.org/10.3390/nano9030483.
[30] I. Manavitehrani, A. Fathi, A. Schindeler, F. Dehghani, Sustained protein release from a core-shell drug carrier system comprised of mesoporous nanoparticles and an injectable hydrogel, Macromol. Biosci. 18 (2018) 1–9, https://doi.org/10.1002/mabi.201800201.
[31] R. Aquino-Martínez, N. Artigas, B. Gámez, J. Luis Rosa, F. Ventura, J.J. Cray, Extracellular calcium promotes bone formation from bone marrow mesenchymal stem cells by amplifying the effects of BMP-2 on SMAD signalling, PloS One 12 (2017) 1–14, https://doi.org/10.1371/journal.pone.0178158.
[32] G.M. Luz, J.F. Mano, Preparation and characterization of bioactive glass nanoparticles prepared by sol-gel for biomedical applications, Nanotechnology 22 (2011) 494014, https://doi.org/10.1088/0957-4484/22/49/494014.
[33] X. Zhou, W. Feng, K. Qiu, et al., BMP-2 derived peptide and dexamethasone incorporated mesoporous silica nanoparticles for enhanced osteogenic differentiation of bone mesenchymal stem cells, ACS Appl. Mater. Interfaces 7 (2015) 15777–15789, https://doi.org/10.1021/acsami.5b02636.
[34] J.M. Oliveira, R.A. Sousa, N. Kotobuki, et al., The osteogenic differentiation of rat bone marrow stromal cells cultured with dexamethasone-loaded carboxymethylchitosan/poly(amidoamine) dendrimer nanoparticles, Biomaterials 30 (2009) 804–813, https://doi.org/10.1016/j.biomaterials.2008.10.024.
[35] H.D.M. Follmann, O.N. Oliveira, D. Lazarin-Bidóia, et al., Multifunctional hybrid aerogels: hyperbranched polymer-trapped mesoporous silica nanoparticles for sustained and prolonged drug release, Nanoscale 10 (2018) 1704–1715, https://doi.org/10.1039/c7nr08464a.
[36] S. Nadine, S.G. Patrício, C.R. Correia, J.F. Mano, Dynamic microfactories co-encapsulating osteoblastic and adipose-derived stromal cells for the biofabrication of bone units, Biofabrication 12 (2019), 015005, https://doi.org/10.1088/1758-5090/ab3e16.
[37] T. Ribeiro, A.S. Rodrigues, S. Calderon, A. Fidalgo, J.L.M. Gonçalves, V. André, M. Teresa Duarte, P.J. Ferreira, J.P.S. Farinha, C. Baleizão, Silica nanocarriers with user-defined precise diameters by controlled template self-assembly, J. Colloid Interface Sci. 561 (2020) 609–619, https://doi.org/10.1016/j.jcis.2019.11.036.
[38] M.T. Tavares, M.B. Oliveira, V.M. Gaspar, J.F. Mano, J.P.S. Farinha, C. Baleizão, Efficient single dose induction of osteogenic differentiation of stem cells using multi-bioactive hybrid nanocarriers, Adv. Biosys (2020) 2000123, https://doi.org/10.1002/adbi.202000123.
[39] M.T. Tavares, M.B. Oliveira, J.F. Mano, J.S.P. Farinha, C. Baleizão, Bioactive silica nanoparticles with calcium and phosphate for a single dose osteogenic differentiation, Mater. Sci. Eng. C 107 (2020) 110348, https://doi.org/10.1016/j.msec.2019.110348.
[40] J.C. Almeida, A. Wacha, P.S. Gomes, et al., A biocompatible hybrid material with simultaneous calcium and strontium release capability for bone tissue repair, Mater. Sci. Eng. C 62 (2016) 429–438, https://doi.org/10.1016/j.msec.2016.01.083.
[41] P. Lavrador, V.M. Gaspar, J.F. Mano, Bioinstructive naringin-loaded micelles for guiding stem cell osteodifferentiation, Adv Healthc Mater 1800890 (2018) 1–16, https://doi.org/10.1002/adhm.201800890.
[42] A. El-Fiqi, J.H. Kim, H.W. Kim, Osteoinductive fibrous scaffolds of biopolymer/mesoporous bioactive glass nanocarriers with excellent bioactivity and long-term delivery of osteogenic drug, ACS Appl. Mater. Interfaces 7 (2015) 1140–1152, https://doi.org/10.1021/am5077759.
[43] Q. Zhang, M. Qin, X. Zhou, et al., Porous nanofibrous scaffold incorporated with S1P loaded mesoporous silica nanoparticles and BMP-2 encapsulated PLGA microspheres for enhancing angiogenesis and osteogenesis, J. Mater. Chem. B 6 (2018) 6731–6743, https://doi.org/10.1039/c8tb02138d.
[44] X. Zhou, W. Weng, B. Chen, et al., Mesoporous silica nanoparticles/gelatin porous composite scaffolds with localized and sustained release of vancomycin for treatment of infected bone defects, J. Mater. Chem. B 6 (2018) 740–752, https://doi.org/10.1039/c7tb01246b.